35th Annual International Conference of the IEEE EMBS
Osaka, Japan, 3 - 7 July, 2013

Performance of a 6-Degree-of-Freedom Active Microsurgical Manipulator in Handheld Tasks

Sungwook Yang, Trent S. Wells, Robert A. MacLachlan, and Cameron N. Riviere

Abstract—This paper presents the first experimental results from human users of a new 6-degree-of-freedom handheld micromanipulator. This is the latest prototype of a fully-handheld system, known as "Micron," which performs active compensation of hand tremor for microsurgery. The manipulator is a miniature Gough-Stewart platform incorporating linear ultrasonic motors that provide a cylindrical workspace 4 mm long and 4 mm wide. In addition, the platform allows the possibility of imposing a remote center of motion for controlling motion not only at the tip but also at the entry point in the sclera of the eye. We demonstrate hand tremor reduction in both static and dynamic micromanipulation tasks on a rubber pad. The handheld performance is also evaluated in an artificial eye model while imposing a remote center of motion. In all cases, hand tremor is significantly reduced.

I. Introduction

Robotic surgical systems have increasingly been a subject of research in microsurgery over the past two decades since they offer various advantages over conventional techniques [1, 2]. For example, such robotic platforms can reduce hand tremor and enable fine manipulation with high precision and dexterity. Most of the platforms are mechanically-grounded robots such as Da Vinci Surgical System, which is teleoperated from a remote console. These systems provide tremor suppression largely through motion scaling, i.e., reducing the amplitude of the surgeon's voluntary hand motion. Teleoperated systems entail certain disadvantages, such as a steep learning curve [2]. Moreover, the lack of direct force feedback to operators can be a significant problem in delicate surgery [3]. Ophthalmic surgery is demanding because it requires fine motor control in a limited working space with high magnification through a surgical microscope [2]. Any error in position can cause collateral damage, resulting in vision loss.

This has led to the development of a cooperative robot, the Steady Hand, utilizing shared control [4, 5]. The robot selectively complies based on force/torque sensor feedback, allowing voluntary motion and suppressing tremor while a surgeon simultaneously holds the surgical instrument. However, due to the mechanical stiffness and inertia of the multiple-degree-of-freedom (DOF) stages, it produces a different feel from that experienced in natural hand motion [6].

Research supported by the U.S. National Institutes of Health (grant nos. R01EB007969 and R01EB000526) and the Kwanjeong Educational Foundation.

S. Yang, R. A. MacLachlan, and C. N. Riviere are with the Robotics Institute, Carnegie Mellon University, Pittsburgh, PA 15213 USA (e-mail: swyang@cmu.edu).

T. S. Wells is with the Department of Biomedical Engineering, Carnegie Mellon University, Pittsburgh, PA 15213 USA.

An alternative to approaches that use table-mounted platforms is a fully-handheld micromanipulator, Micron, developed for intraocular surgery and cell manipulation. The previous prototype features 3-DOF manipulation [3, 7]. It actively stabilizes an end-effector, suppressing tremor while preserving voluntary motion. Despite the advantages of Micron in terms of usability, safety and economy, the 3-DOF system has several drawbacks which must be overcome to enable practical use. The range of motion at the tool tip, for instance, is restricted to a few hundred microns due to the small displacement of piezoelectric bender actuators used [6]. The 3-DOF prototype also cannot offer a remote center of motion (RCM) in manipulation. In particular for ophthalmic surgery, an RCM is necessary in order to avoid unwanted transverse movement at the point of the scleral incision [8].

Therefore, we have proposed a new Micron design having a larger range of motion and increased degrees of freedom in a smaller package using a miniature Gough-Stewart platform. In previous research, the basic design of the new Micron and its optimization were introduced, and a benchtop version was later built to verify the optimization [6]. In this paper, we describe the development of a fully-handheld micromanipulator and present the results of its handheld performance.

II. Methods

A. Handheld Micromanipulator

The active handheld micromanipulator shown in Fig. 1 adopts the Gough-Stewart platform [9] to take advantage of the high stiffness while still occupying a small volume. The parallel link mechanism incorporates six ultrasonic linear motors (SQUIGGLE® SQL-RV-1.8, New Scale Technologies, Inc., USA), which provides 6-DOF motion within a cylindrical workspace 4 mm in diameter and 4 mm long. A bearing assembly was devised to decouple the pure linear motion from the rotational motion of the motors. Each

Figure 1. 6 DOF Micron, an active handheld micromanipulator.

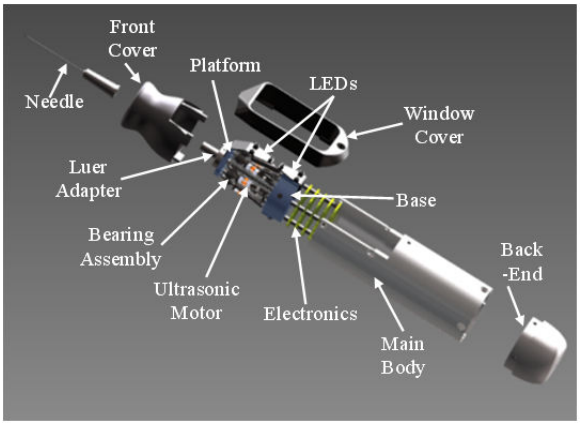

Figure 2. Exploded view of handheld micromanipulator assembly.

bearing assembly contains a linear actuator module and bearing. The upper and lower ends are connected to the moving platform and the base by flexures (#1-0 polypropylene suture) as shown in Fig. 2. The mechanism has an overall diameter of 23 mm and a height of 37 mm. These dimensions have been optimized to allow maneuverability in the desired cylindrical workspace while withstanding side loads up to 200 mN [6].

The manipulator is also equipped with infrared LEDs to detect the position and orientation of both the tool tip and the handle. Three LEDs are mounted to the platform and three are affixed to the handle (the LEDs are visible as small white blocks in Fig. 1). A custom-built microscale optical tracking system, ASAP (Apparatus to Sense Accuracy of Position), senses the differently modulated signals on each LED and converts them to position and orientation at a sampling rate of 1 kHz over a 27 cm^3 workspace, with less than 10 µm RMS noise [10].

The manipulator includes a male Luer-Slip adaptor to accommodate a variety of end-effectors. A PCB stack of five layers is attached to the bottom of the platform base. The three layers of the PCB stack closest to the base drive the motors, which communicate with a main controller via inter-integrated circuit (I^2C) protocol. The remaining two layers on the bottom are used for driving the LEDs. The handle is composed of four pieces: a front cover, a window cover, a main body, and a back end. The front cover was designed to provide an ergonomic grip and manufactured by CNC machining. The window cover and the back end are fabricated by rapid prototyping. The outer diameter of the instrument is 28.5 mm. The length is 126 mm, excluding any end-effector attached to the Luer-Slip adaptor. Fig. 1 presents the fully assembled manipulator.

B. Active Tremor Cancellation

Two alternatives for tremor filtering have been designed for error canceling in Micron [3]. The first is a lowpass filter with a corner frequency of 1.5 Hz. Since voluntary motion typically occurs below 2 Hz, the filter has unity gain before the corner frequency and high attenuation beyond 10 Hz in order to stabilize the instrument tip. The second alternative is a lowpass shelving filter which provides what may be considered relative motion scaling. The shelving filter features unity gain below 0.15 Hz, and gain of about 1/3 for the frequency range of 0.15 Hz to 2 Hz, with high attenuation beyond 2 Hz.

C. Testing

In order to accurately assess the handheld performance of Micron, static and dynamic tasks were performed on a laser engraved rubber target under a board-approved protocol. The effect of Micron on cancelling tremor during static conditions was examined through a holding-still task. A participant was asked to locate the tip of the instrument a distance directly above a target defined on the rubber pad, then to maintain the same tip position for a 20 second duration in each trial.

A circle-tracing task was used to examine dynamic tremor cancellation. The participant was instructed to trace a 500 µm diameter circle as accurately as possible on a rubber pad for 20 seconds while maintaining a constant height above the pad. Each activity was repeated for three modes: unaided (no cancellation), lowpass filtering, and motion scaling. The participant performed five trials for each task/mode combination. This resulted in six different task/mode combinations. During the five trials the combinations were varied using a Latin square design to prevent bias from repeatedly performing the same task.

Five holding-still trials were also conducted for each of the three control modes within an artificial eye model (referred to as the 'eye phantom') for 10 seconds duration. The eye phantom was developed by Johns Hopkins University and consists of a hollow 25 mm diameter sphere molded from soft silicone to mimic the natural sclera. The eye phantom was allowed to freely rotate in a ball cup treated with water based lubricant (K-Y® jelly) as shown in Fig. 3. During the task, a 27 Gauge needle was inserted into the eye phantom through a cannula placed in the side wall, imposing an RCM constraint on the needle.

All tasks were performed under magnification (Zeiss® OPMI™ surgical microscope) and video was collected at 30Hz through stereo cameras attached to the microscope as shown in Fig. 3. The trajectory of the tool tip was overlaid on the video through custom software. 3D position data was also collected using ASAP. An algorithm was then used to align the 3D data set such that the axis corresponded to the microscope viewing plane.

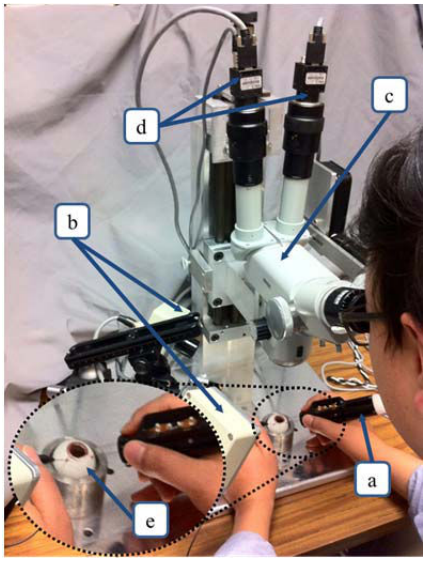

Figure 3. Experimental setup. (a) Micron, (b) ASAP, (c) microscope, (d) CCD camera, and (e) eye phantom.

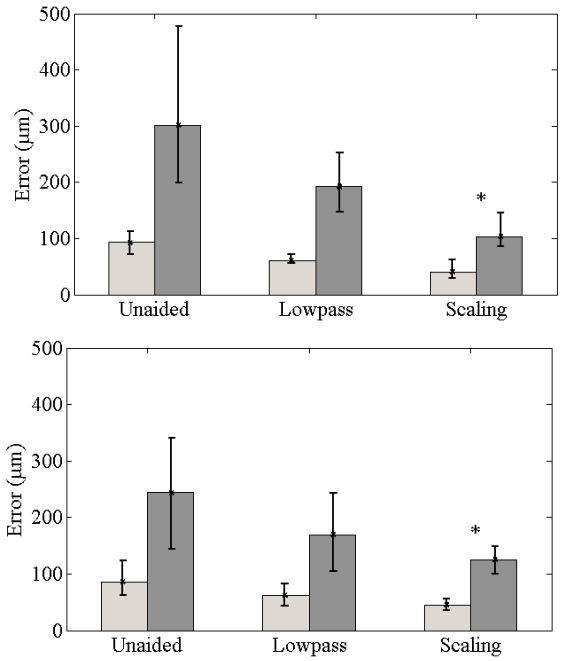

Figure 4. Average RMS (light gray) and maximum (dark gray) errors for holding-still (top) and circle-tracing (bottom) tasks. Error bars indicate maximum and minimum values over 5 trials for each control mode. Scaling mode significantly reduces the errors compared to unaided trials for both holding-still and circle-tracing.

III. Results

The roots mean square error (RMSE) and the maximum error (ME) were evaluated across trials for each control mode (unaided, lowpass, and scaling). Evaluating the RMSE is useful for the design of the instrument and examining its overall performance. However, the maximum error may be found to be more relevant to surgical applications as even one deviation outside of the desired workspace can cause substantial damage to surrounding tissue structures. Fig. 4 and Fig. 7 present RMSE (light gray bar) and ME (dark gray bar) averaged across all trials for each individual mode. The error bars in the figures indicate minimum and maximum values over the five trials for each control mode.

A. Rubber Target: Holding-Still

As shown in Fig. 4 (top), both RMSE and ME are reduced in aided trials such as lowpass and scaling. The RMSE and ME of lowpass mode are roughly 65% of the unaided trials. The scaling mode shows a statistically significant (p = 0.003) reduction of the average maximum error to 34% of unaided maximum error. Scaling mode is shown to be most effective during the holding-still task, despite the primary intention of the control mode to scale down gross motion of the tool tip during dynamic tasks. This may be due to an ability of the scaling modes to cancel erroneous motion driven by eye-hand feedback.

TABLE I
Comparison of 3D RMS and Maximum Errors

Condition	Control	RMSE (μm)	ME (μm)
Rubber target (Holding-still)	Unaided	93 (100.0 %)	301 (100.0 %)
	Lowpass	61 (65.6 %)	192 (63.9 %)
	Scaling	40 (43.6 %)	103 (34.3 %)
Rubber target (Circle-tracing)	Unaided	86 (100.0 %)	244 (100.0 %)
	Lowpass	62 (71.8 %)	170 (69.5 %)
	Scaling	45 (52.6 %)	125 (51.2 %)
Eye phantom (Holding-still)	Unaided	204 (100.0 %)	573 (100.0 %)
	Lowpass	174 (85.3 %)	413 (72.0 %)
	Scaling	117 (57.6 %)	282 (49.2 %)

RMSE = root mean square error, and ME = maximum error.
The values in parentheses indicate percentages of average error with respect to the average error of unaided trials.

B. Rubber Target: Circle-tracing

The circle-tracing task was analyzed by obtaining a best correlation of the data with a 500 μm circle located in a plane parallel to the viewing plane through the microscope. Errors were calculated by comparing the distance between each point and the nearest point on the circle. Error for the circle-tracing task followed a similar trend to the holding-still task as shown in Fig. 4 (bottom). ME in lowpass mode was reduced to an average of 70% of unaided ME. ME in scaling mode was 51% of unaided ME. The reduction in the scaling mode was statistically significant (p = 0.02).

Depth perception is known to be hampered when performing procedures through a surgical microscope [11]. The additional benefit of scaling mode during circle-tracing is illustrated in Fig. 5 by the noticeable reduction of error along the viewing depth or z-axis. In unaided cases RMSE in z-axis motion is 123% greater than motion within the transverse x-y plane. In lowpass mode the RMSE in z-axis motion is reduced to 93%, and reduced slightly more to 91% during scaling mode, as compared to RMSE in the transverse plane.

C. Eye Phantom: Holding-Still

Although the hold still task in the eye phantom is similar to

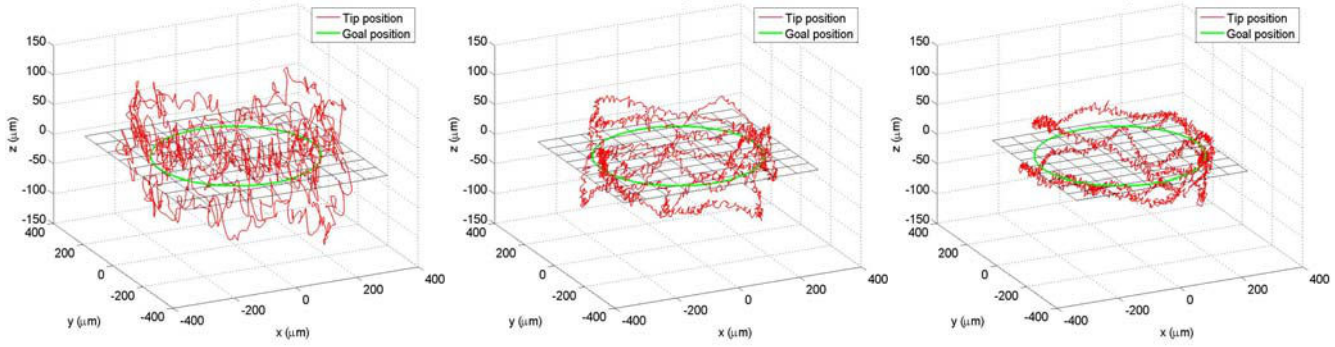

(a) (b) (c)

Figure 5. Result of circle-tracing task according to three control modes. Red lines depict the trajectory of the tool tip for 20 seconds. (a) Unaided (off) trial, (b) aided trial with lowpass, (c) aided trail with scaling mode.

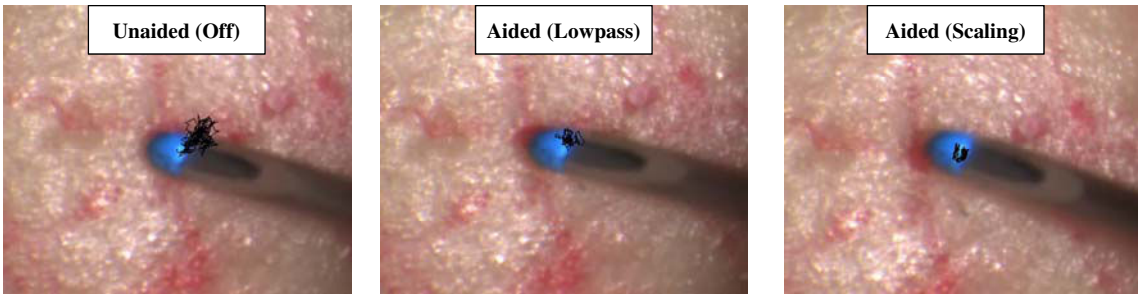

(a) (b) (c)

Figure 6. Result of hold still task in an eye phantom. Black lines depict the trajectory of the tool tip for 10 seconds. (a) Unaided (off) trial, (b) aided trial with lowpass, (c) aided trail with scaling mode.

the rubber target version, the difficulty is greater due to the awkward kinematics. This includes the fulcrum imposed by the phantom, as well as the rotation of the eye phantom due to voluntary motion and/or tremor.

Fig. 6 shows the tip trajectory (black trace) overlaid on the recorded video clip for 10 seconds for each of the three control modes. Tremor compensation was found to decrease positioning error in the eye phantom similar to rubber target tasks. The scaling mode produced significantly lower error than the unaided mode (p = 0.001). The quantitative results are also summarized in Table I.

IV. Discussion

We demonstrate the first handheld performance of the newly developed 6-DOF Micron to improve positioning accuracy by reducing tremor. It is found that the 6-DOF Micron provides a statistically significant reduction in 3D positioning error. The new design offers an order-of-magnitude increase in range of motion using the novel linear actuators. As a result, the tremor reduction is improved along the viewing axis, while remaining comparable to the 3-DOF system within the transverse viewing plane [3]. In addition to positioning improvements, an RCM constraint has been implemented to enable proper operation within an eye phantom.

The benefit of the larger range of motion in the new 6-DOF Micron extends the capabilities beyond tremor reduction. Additional control may be applied to accomplish versatile handheld operations in microsurgery such as endoscopic optical coherence tomography imaging [12] and semi- or fully-automatic laser surgery [13].

In order to achieve higher positioning accuracy and tremor reduction, the control bandwidth of the manipulator should be increased. It is currently limited by a chattering instability in the range of 50-100 Hz. Therefore, future work involves refinement of the micromanipulator design and control. Further experiments will also be performed on various tasks *ex vivo* and *in vivo* with multiple subjects in order to rigorously confirm the handheld performance improvement.

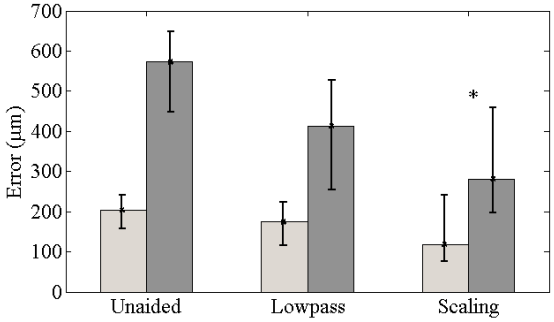

Figure 7. Average RMS (light gray) and maximum (dark gray) errors for holding-still task in an eye phantom. Error bars indicate maximum and minimum values among the maximum errors over 5 trials for each control mode. Statistical significance is marked with an asterisk in the scaling mode.

References

[1] G. Dogangil, B. L. Davies, and F. Rodriguez y Baena, "A review of medical robotics for minimally invasive soft tissue surgery," Proc. Inst. Mech. Eng. H, vol. 224, pp. 653-79, May 2010.

[2] J. D. Pitcher, J. T. W. Wilson, T. C. Tsao, S. D. Schwartz, and J. P. Hubschman, "Robotic Eye Surgery: Past, Present, and Future," J. Comput. Sci. Syst. Biol., vol. 3, pp. 1-4, 2012.

[3] R. A. MacLachlan, B. C. Becker, J. C. Tabarés, G. W. Podnar, J. Louis A. Lobes, and C. N. Riviere, "Micron: an actively stabilized handheld tool for microsurgery," IEEE Trans. Robot., vol. 28, pp. 195-212, Feb. 2012.

[4] R. Taylor, P. Jensen, L. Whitcomb, A. Barnes, R. Kumar, Stoianovici, D. Gupta, Wang, E. De Juan, and L. Kavoussi, "A Steady-Hand robotic system for microsurgical augmentation," Int. J. Robot. Res., vol. 1679, pp. 1201-1210, Dec. 1999.

[5] B. Mitchell, J. Koo, M. Iordachita, P. Kazanzides, A. Kapoor, J. Handa, G. Hager, and R. Taylor, "Development and application of a new Steady-Hand manipulator for retinal surgery," in Proc. IEEE Int. Conf. Robot. Autom., 2007, pp. 623-629.

[6] S. Yang, R. A. MacLachlan, and C. N. Riviere, "Design and analysis of 6 DOF handheld micromanipulator," in Proc. IEEE Int. Conf. Robot. Autom., 2012, pp. 1946-1951.

[7] J. Cuevas Tabarés, R. A. Maclachlan, C. A. Ettensohn, and C. N. Riviere, "Cell micromanipulation with an active handheld micromanipulator," in Proc. 32nd Annu. Int. Conf. IEEE. Eng. Med. Biol. Soc., 2010, pp. 4363-4366.

[8] P. S. Jensen, K. W. Grace, R. Attariwala, J. E. Colgate, and M. R. Glucksberg, "Toward robot-assisted vascular microsurgery in the retina," Graefes Arch. Clin. Exp. Ophthalmol., vol. 235, pp. 696-701, 1997.

[9] V. E. Gough, "Contribution to discussion of papers on research in automobile stability, control and tyre performance," Proc. Auto Div. Inst. Mech. Eng., vol. 171, pp. 392-395, 1956.

[10] R. A. MacLachlan and C. N. Riviere, "High-speed microscale optical tracking using digital frequency-domain multiplexing," IEEE Trans. Instrum. Meas., vol. 58, pp. 1991-2001, Jun. 2009.

[11] L. T. Du, I. F. Wessels, J. P. Underdahl, and J. D. Auran, "Stereoacuity and depth perception decrease with increased instrument magnification: comparing a non-magnified system with lens loupes and a surgical microscope," Binocul. Vis. Strabismus Q., vol. 16, pp. 61-67, 2001.

[12] S. Yang, M. Balicki, R. A. MacLachlan, L. Xuan, J. U. Kang, R. H. Taylor, and C. N. Riviere, "Optical coherence tomography scanning with a handheld vitreoretinal micromanipulator," in Proc. 34th Annu. Int. Conf. IEEE Eng. Med. Biol. Soc., 2012, pp. 948-951.

[13] B. C. Becker, R. A. MacLachlan, L. A. Lobes Jr, and C. N. Riviere, "Semiautomated intraocular laser surgery using handheld instruments," Lasers Surg. Med., vol. 42, pp. 264-273, 2010.